

COMBINED EXPERIMENTAL AND THEORETICAL STUDY OF STABILITY OF La_2Ni_7

¹Ondřej ZOBAČ, ¹Martin FRIÁK, ^{1,2}Sabina KOVAŘÍKOVÁ OWEIS, ^{1,2}Jana PAVLŮ, ³David HOLEC,
⁴Simona ZLÁ, ⁴Monika KAWULOKOVÁ, ⁴Bedřich SMETANA, ⁵Andy WATSON

¹*Institute of Physics of Materials, v.v.i., Czech Academy of Sciences, Brno, Czech Republic, EU,
zobac@ipm.cz; friak@ipm.cz; kovarikova@ipm.cz,*

²*Department of Chemistry, Faculty of Science, Masaryk University, Brno, Czech Republic; EU,
houserova@chemi.muni.cz*

³*Department of Materials Science, Montanuniversität Leoben, Franz-Josef-Straße 18, Leoben, A-8700,
Austria, EU, david.holec@unileoben.ac.at*

⁴*VSB - Technical University of Ostrava, Ostrava, Czech Republic, EU, simona.zla@vsb.cz,
monika.kawulokova@vsb.cz, bedrich.smetana@vsb.cz*

⁵ *Hampton Thermodynamics Limited, Hampton. United Kingdom, andywatson7@gmail.com*

"DOI - will be assigned by the organizer."

Abstract

The La-Ni binary system, and in particular the LaNi_5 binary intermetallic phase, has been intensively studied in recent decades, especially as a promising hydrogen storage material. Knowledge of phase equilibria is very important for the possible optimization of material properties. This work is focused on the study of the thermodynamic properties of the La_2Ni_7 phase, which occurs in phase equilibrium with the LaNi_5 phase and can therefore influence the capacity and dynamics of these hydrogen storage materials in real materials. The alloy samples were prepared from pure elements using a gravity melting furnace in an inert Ar-6N atmosphere. The overall composition and chemical composition of the phases were analyzed by SEM-EDX. The crystal structure of the phases was confirmed by powder XRD. Our experiments were complemented by quantum-mechanical calculations implementing the density functional theory (DFT) within the generalized gradient approximation (GGA) to determine the ground-state structural, electronic, thermodynamic, and elastic properties of La_2Ni_7 . A computational unit cell of La_2Ni_7 contains 36 atoms and has a strongly anisotropic shape. The computed results obtained for static lattices indicate that La_2Ni_7 is thermodynamically stable with respect to the decomposition into elemental end members. The stress-strain method was used to address the mechanical stability by computing a full tensor of the second-order elastic constants and La_2Ni_7 has been found to be mechanically stable.

Keywords: La-Ni, quantum-mechanical calculations, stability, thermodynamics, elasticity

1. INTRODUCTION

The La-Ni binary system has been intensively studied for decades for its potential use as a hydrogen storage material. [1]. The hydrogen sorption and desorption properties can be effectively optimized by using a mixture of phases or by adding a third element [2]. Knowledge of phase equilibria can be advantageously used in optimizing the composition and coexistence of phases at given temperatures.

Nine phases can be found in binary system **La-Ni** [3]: La_3Ni (crystal structure Fe_3C , oP16-Pnma), La_7Ni_3 , (structure type Fe_3Th_7 , hP20-P63/mc), LaNi (structure type CrB, oS8-Cmcm), $\text{La}_7\text{Ni}_{16}$ (structure type $\text{La}_7\text{Ni}_{16}$, tI46-I-42m), La_2Ni_3 (structure type La_2Ni_3 , oS20-Cmca), LaNi_3 (structure type PuNi_3 , hR36-R-3m), $\alpha\text{-La}_2\text{Ni}_7$ (structure type Ce_2Ni_7 , hP36-P63/mmc), $\beta\text{-La}_2\text{Ni}_7$ (structure type Gd_2Co_7 , hR54-R-3m), $\text{La}_5\text{Ni}_{19}$ (structure type $\text{Pr}_5\text{Co}_{19}$ ($\text{Sm}_5\text{Co}_{19}$), hP48-P63/mmc), LaNi_5 (structure type CaCu_5 , hP6-P6/mmm).

The binary phase of LaNi_5 is known to form relatively stable LaNi_5H_x hydrides when reacted with hydrogen. The presence of other phases can affect the thermodynamic and kinetic properties of this reaction. The stability of the closest phase $\text{La}_5\text{Ni}_{19}$ is not clearly described in the literature. Ye et al. consider it to be stable in the temperature range RT-1004.5 [4] based on older experimental work.

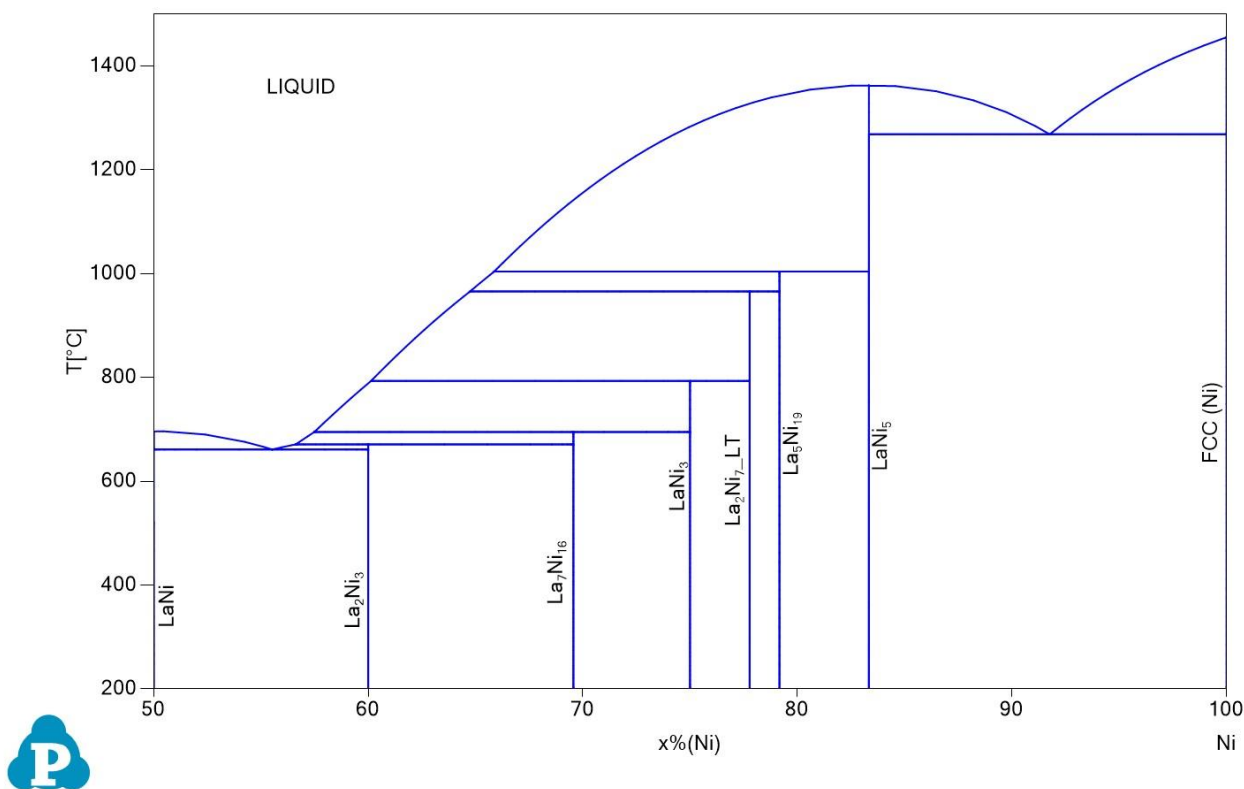


Figure 1: Phase diagram La-Ni proposed by Ye [4] includes $\text{La}_5\text{Ni}_{19}$ binary phase

2. EXPERIMENTAL STUDY

The overall composition of the experimental sample was chosen with the main aim of describing the LaNi_5 phase and its surrounding. Sample as prepared from pure elements using a vacuum gravity furnace under an inert atmosphere of Ar-6N. The casted alloy was analyzed and characterized by a combination of analytical methods. Overall and phase chemical composition was measured by scanning electron microscopy with energy dispersive X-ray detector (SEM-EDX). Microstructure of casted sample is presented in Figure 2.

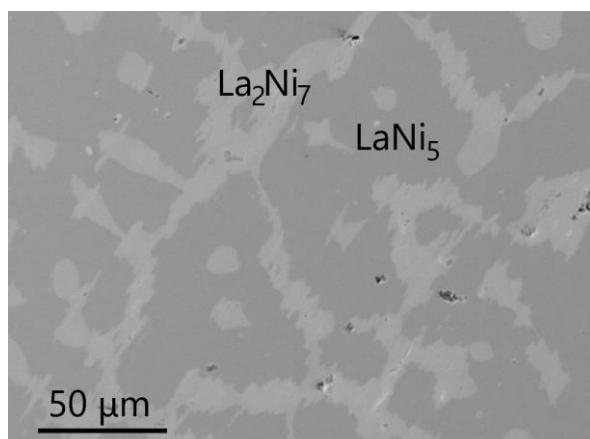


Figure 2: Microstructure of the casted sample La-Ni consisting of LaNi_5 and La_2Ni_7 phases.

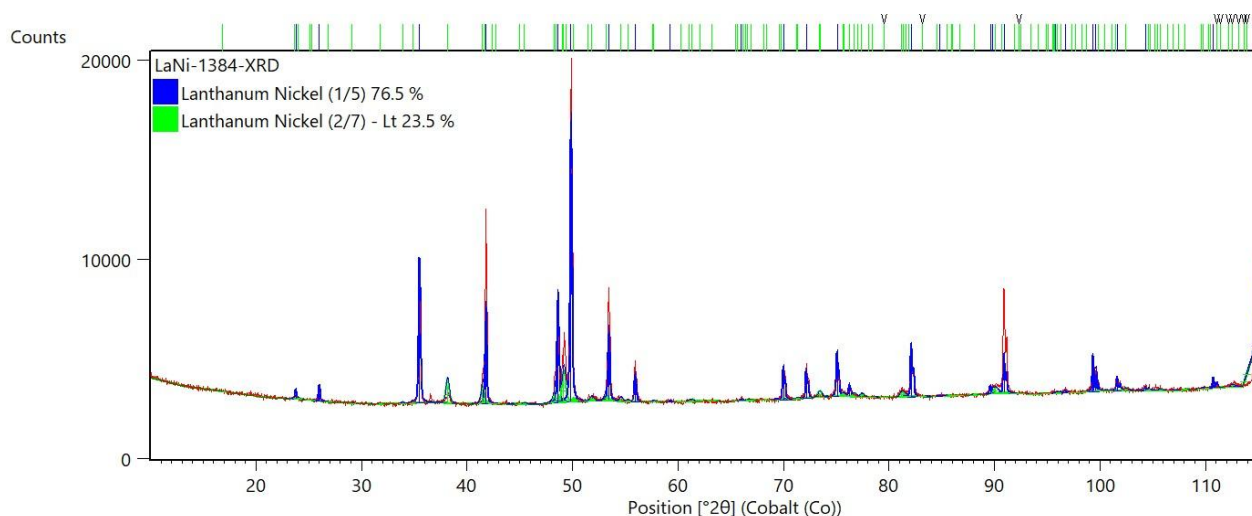


Figure 3: XRD pattern of the casted sample LaNi consisting of 76.5% LaNi_5 and 23.5% La_2Ni_7 phases. Measured diffractogram shown in red, calculated pattern refined with the Rietveld method for LaNi_5 shown in blue and La_2Ni_7 in green.

Crystallographic structures of found phases were confirmed by powder X-ray diffraction (XRD) with the XRD pattern shown in Figure 3. The information obtained on the structure analysis of the casted samples shows that the La_2Ni_7 phase appears to be kinetically stable in coexistence with the LaNi_5 phase. Thermodynamic stability will be studied in future work using long-term annealed samples.

3. COMPUTATIONAL METHODOLOGY

Regarding our first-principles calculations, we employed the Vienna Ab initio Simulation package (VASP) [5,6] that implements the density functional theory (DFT) [7,8] using projector augmented waves (PAW) [9,10] (pseudo-)potentials. In particular, an 11-valence-electron La potential (core=Kr4d) and 16-valence-electron Ni_pv potential from the potpaw_PBE.52 VASP database were used. The exchange-correlation energy was parametrized within the generalized gradient approximation (GGA) by Perdew, Burke and Ernzerhof (PBE'96) [11]. The plane-wave energy cut-off was set to 520 eV. We applied the Methfessel-Paxton smearing scheme of order 1 with the smearing parameter set to 0.05. The non-spherical contributions related to the gradient of the density in the PAW spheres were included (the LASPH parameter was set to TRUE). An additional support grid was used for the evaluation of the augmentation charges (the ADDGRID parameter was set to TRUE). Due to the fact that the 36-atom computational unit cell of the crystal structure of La_2Ni_7 is highly shape-anisotropic (with the ratio of the hexagonal-lattice parameters c/a close to 5, see Fig. 4), its reciprocal space unit cell was sampled by $10 \times 10 \times 2$ k-points. Single-crystal elastic constants were computed employing the stress-strain method [12].

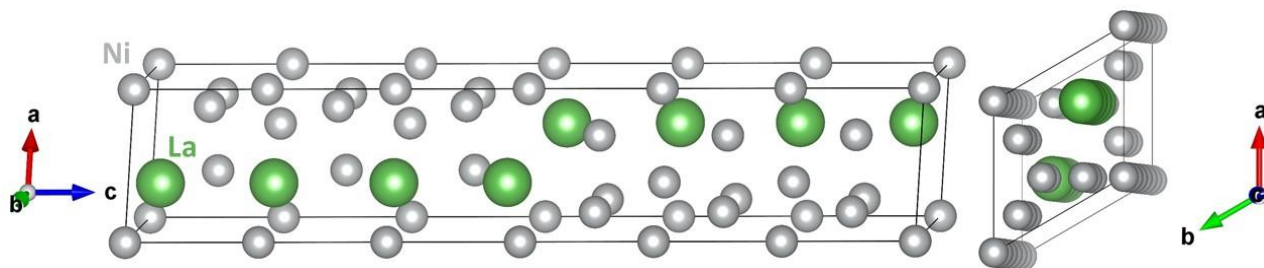


Figure 4 Schematic visualization of the 36-atom computational unit cell of crystal structure of La_2Ni_7 .

4. RESULTS

Our calculations started with identifying the ground-state structure of the studied La_2Ni_7 by fully relaxing the computational unit cell of La_2Ni_7 shown in Fig. XX1. The full relaxation proceeded by minimizing the energy of the static lattice with respect to the volume, cell shape as well as the atomic positions. The equilibrium lattice parameters were computed equal to $a = 5.023 \text{ \AA}$ and $c = 24.578 \text{ \AA}$. The ground state was found magnetic with the total magnetic moment equal to $0.97 \mu_B$ per 9-atom formula unit of La_2Ni_7 with the spin-polarization mostly associated with the Ni atoms.

In order to address the thermodynamic stability of the studied La_2Ni_7 , we evaluated its formation energy ΔE_f using its mathematical expression as follows:

$$\Delta E_f(\text{La}_2\text{Ni}_7) = \frac{(E(\text{La}_2\text{Ni}_7) - 2 * E(\text{La}) - 7 * E(\text{Ni}))}{2 + 7},$$

where we employed the static-lattice energy $E(\text{La}_2\text{Ni}_7)$ of the La_2Ni_7 intermetallic compound and energies of constituting pure elements in their ground-state structures. In particular, $E(\text{La})$ stands for the non-magnetic hexagonal close-packed structure of La and $E(\text{Ni})$ for the ferromagnetic face-centred-cubic (fcc) Ni. The computed formation energy is equal to -0.316 meV/atom . Its negative value indicates that La_2Ni_7 is stable with respect to the decomposition into elemental end members.

In order to evaluate the mechanical stability of La_2Ni_7 we determined a full-tensor of single-crystal elastic constants using the stress-strain method [12]. The elastic constants are below (in GPa) as a 6x6 matrix:

191	110	83	0	0	0
110	190	83	0	0	0
83	83	207	0	0	0
0	0	0	47	0	0
0	0	0	0	47	0
0	0	0	0	0	40

The computed single-crystal elastic properties of La_2Ni_7 are visualized in the form of directional dependences of Young's modulus and the linear compressibility in Fig. 5 employing the ELATE software [13] (open-access online at <https://progs.coudert.name/elate>). As seen in Fig.5, the La_2Ni_7 is not strongly elastically anisotropic.

A system is considered mechanically stable if all the eigenvalues of its 6x6 matrix of the single-crystal elastic constants are positive. We used the ELATE software to determine these eigenvalues and we got the following eigenvalues: 40, 47, 47, 80, 128, 380 (all in GPa). As they are all positive, the La_2Ni_7 is computed mechanically stable. Further, using the ELATE software, we also homogenized the single-crystal elastic constants according to three homogenization methods (Voigt, Reuss, Hill) and predicted selected polycrystal characteristics (bulk modulus, Young's modulus, shear modulus and Poisson's ratio). Their values are summarized in Table 1.

Table 1 Homogenized elastic characteristics (bulk modulus, Young's modulus, shear modulus and Poisson's ratio) according to Voigt's, Reuss' and Hill's homogenization methods as evaluated by the ELATE software tool [13] (open-access online at <https://progs.coudert.name/elate>).

homogenization method	bulk modulus (GPa)	Young's modulus (GPa)	shear modulus (GPa)	Poisson's ratio (-)
Voigt	127	127	48	0.3327
Reuss	127	124	46	0.3369
Hill	127	125	47	0.3348

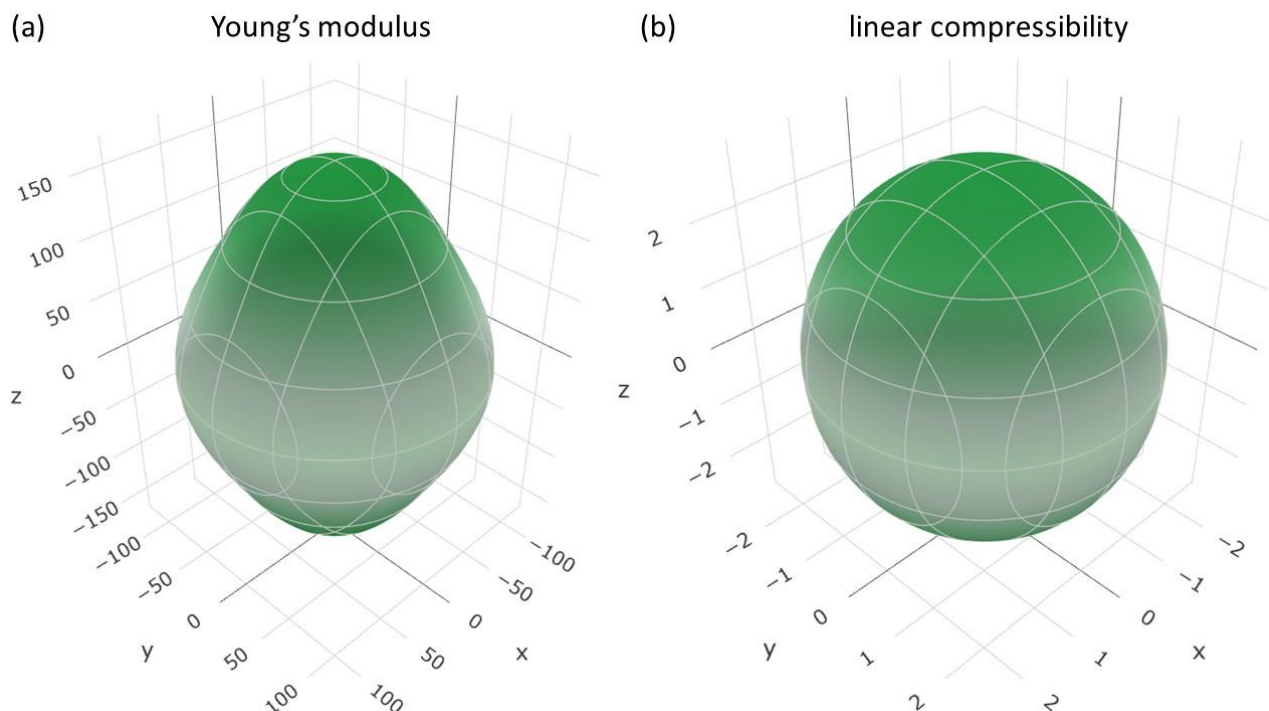


Figure 5 Directional dependences of Young's modulus (a) and the linear compressibility (b) as visualizations of the single-crystal elastic properties of La_2Ni_7 . The visualization was done by the ELATE software [13] (open-access online at <https://progs.coudert.name/elate>).

5. CONCLUSION

Experimental study of the casted alloys shows that the phase La_2Ni_7 is formed during quenching together with the binary phase LaNi_5 . Existence of this phase was confirmed by SEM-EDX and XRD analytical methods. Thermodynamic stability will be analyzed from long-term annealed samples in our future research. As a complement to our experiments, we have also performed a series of quantum-mechanical calculations. The static-lattice ground-state structure of La_2Ni_7 was found by full relaxation, and its thermodynamic and mechanical stability was assessed. The formation energy of La_2Ni_7 was found negative (equal to -0.316 meV/atom) and La_2Ni_7 is, therefore, computed to be thermodynamically stable with respect to the decomposition into elemental end members La and Ni. Next, a full tensor of single-crystal elastic constants was determined using the stress-strain method. As all its eigenvalues are positive, we found La_2Ni_7 mechanically stable.

ACKNOWLEDGEMENTS

This study is a part of the project No. CZ.02.01.01/00/22_008/0004631 Materials and technologies for sustainable development within the Jan Amos Komensky Operational Program financed by the European Union and from the state budget of the Czech Republic. DH acknowledges the financial support by the Austrian Federal Ministry for Labour and Economy and the Christian Doppler Research Association. Computational resources were made available by the Ministry of Education, Youth and Sports of the Czech Republic under the Project e-INFRA CZ (ID:90254) at the IT4Innovations National Supercomputing Center, the MetaCentrum and CERIT-SC. Access to the CERIT-SC computing and storage facilities provided by the CERIT-SC Center, under the programme "Projects of Large Research, Development, and Innovations Infrastructures" (CERIT Scientific Cloud LM2015085) and access to CESNET storage facilities provided by the project "e-INFRA CZ" under the

programme “Projects of Large Research, Development, and Innovations Infrastructures” LM2023054) is acknowledged. The computational cell in Figure 4 was visualized using the VESTA package [14].

6. SUPPLEMENTARY DATA:

The ground-state structure VASP files of La_2Ni_7 are available at DOI: 10.5281/zenodo.15387034

REFERENCES

- [1] Bowman R.C., Witham C., Fultz B., Ratnakumar B.V., Ellis, Anderson I.E., Hydriding behavior of gas-atomized AB5 alloys. *J. Alloys Comp.* 1997, vol. 253–254, pp. 613-616.
- [2] Mendelsohn M.H., Gruen D.M., Dwight A.E., $\text{LaNi}_5\text{-xAl}_x$ is a versatile alloy system for metal hydride applications, *Nature* 1977, vol. 269, pp. 45–47.
- [3] Fartushna I., Mardani M., Bajenova I., Khvan A., Cheverikin V., Richter K.W., Kondratiev A., Phase transformations and phase equilibria in the La-Ni and La-Ni-Fe systems. Part 1: Liquidus & solidus projections. *Journal of Alloys and Compounds*. 2020, vol. 845, pp. 156356.
- [4] Ye H., Rong M., Zao Q., Chen Q., Wang J., Rao G., Yhou H., Phase equilibria and thermodynamic properties in the RE-Ni (RE = rare earth metals) binary systems. *J. Mater. Sci.* vol. 58, pp. 1260-1292.
- [5] KRESSE, G., HAFNER, J. Ab initio molecular dynamics for liquid metals. *Physical Review B*, 1996, vol. 47, pp. 558. <https://doi.org/10.1103/PhysRevB.47.558>
- [6] KRESSE, G., FURTHMÜLLER, J. Efficient iterative schemes for ab initio total energy calculations using a plane-wave basis set. *Physical Review B*, 1996, vol. 54, pp. 11169. <https://doi.org/10.1103/PhysRevB.54.11169>
- [7] HOHENBERG, P., KOHN, W. Inhomogeneous electron gas. *Physical Review B*, 1964, vol. 136, pp. B864. <https://doi.org/10.1103/PhysRev.136.B864>
- [8] KOHN, W., SHAM, L. J. Self-consistent equations including exchange and correlation effects. *Physical Review A*, 1965, vol. 140, pp. A1133. <https://doi.org/10.1103/PhysRev.140.A1133>
- [9] BLÖCHL, P. E. Projector augmented-wave method. *Physical Review B*, 1994, vol. 50, pp. 17953. <https://doi.org/10.1103/PhysRevB.50.17953>
- [10] KRESSE, G., JOUBERT, D. From ultrasoft pseudopotentials to the projector augmented-wave method. *Physical Review B*, 1999, vol. 59, pp. 1758. <https://doi.org/10.1103/PhysRevB.59.1758>
- [11] PERDEW, J. P., BURKE, K., ERNZERHOF, M. Generalized gradient approximation made simple. *Physical Review Letters*, 1996, vol. 77, pp. 3865. <https://doi.org/10.1103/PhysRevLett.77.3865>
- [12] ZHOU, L., HOLEC, D., MAYRHOFFER, P.H. Alloying-related trends from first principles: An application to the Ti-Al-X-N system. *Journal of Applied Physics*, 2013, vol. 113, pp. 113510. <https://doi.org/10.1063/1.4795590>
- [13] Romain Gaillac et al., ELATE: an open-source online application for analysis and visualization of elastic tensors *J. Phys.: Condens. Matter* 28 (2016) 275201. DOI 10.1088/0953-8984/28/27/275201
- [14] MOMMA, K., IZUMI, F. VESTA 3 for three-dimensional visualization of crystal, volumetric and morphology data. *Journal of Applied Crystallography*, 2011, vol. 44, pp. 1272. <https://doi.org/10.1107/S0021889811038970>